

Class Project: MAE 272, Spring 2014

Design of a Satellite Attitude Control System

E. Etan Halberg, John Karasinski, and Melanie Stich
University of California, Davis, CA 95616

Abstract

An object in a zero-G or micro-gravity environment, such as a satellite in orbit around Earth, has three translational and three rotational degrees of freedom. In general, it is desirable to have some control over the motion of such a satellite to change or maintain orbit characteristics (i.e. station keeping) or to change or maintain orientation in 3D space (i.e. attitude control). The ability to control a satellite enables many applications, scientific and otherwise, some of which include astrophysics (e.g. deep-space observation), communications (e.g. directional radio transmissions), and proximity operations [15, 16, 18]. A satellite control system utilizes actuators for translational and rotational motion. The highly idealized satellite control system described herein employs one momentum wheel for stability aligned with the pitch axis, and three reaction wheels, one aligned with each of the three primary axes. This system is used for rotational control in order to combat the disturbance forces and torques present in low Earth orbit (LEO).

Controller I/O

The controller requires a set of input angles to maintain or achieve rotational stability or rotational change. An object at or near Earth's surface relies on the ground and Earth's magnetic field as reference for yaw, pitch, and roll, whereas a satellite may not. Instead, satellites rely on other types of sensors for attitude determination. A satellite may rely on measurements taken with respect to relative axes (i.e. its own) – the values for which typically rely on internal gyroscopic mechanisms – or values procured using an absolute reference, such as the Earth, the Sun, or distant stars (e.g. Sun sensors, Earth-horizon sensors, star trackers) or, more typically, both (see Figure 1) [17].

The desired satellite orientation is a user-defined controller input. An additional set of controller inputs may be the rates with which to achieve a desired altitude or orientation, though these should default to controller defined values. Controller inputs not specified by an outside operator include sensor measurements and disturbances. Disturbance inputs are uncontrolled and can include internal noise (e.g. magnetic, vibration), aerodynamic drag, solar

pressure, gravity gradient, magnetic field, space debris, and many others [8]. The controller mediates these disturbances to match the desired user input.

The digital controller is responsible for moderating the power supplied to the plant, which is comprised of three motors and the reaction wheel driven by each. This plant translates power into torque, which becomes angular change through the vehicle dynamics. Thus, angular change is the system output. Through sensor feedback the controller compares each measurable system output to its respective desired value and modifies its own output based on the difference. In addition to angular position the angular rates of change are of interest, as well.

The rate of change in orientation should be approximately zero for stabilization. The rate of change should be non-zero and in the appropriate direction for satellite maneuvers. Several outputs should be monitored within the controller, including the difference between desired orientation and current orientation (i.e. three angle measurements coming from sensors), the rates of change for orientation, and the torques generated by each of the reaction wheels [4].

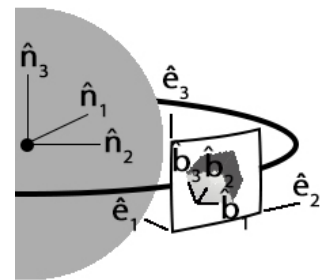


Figure 1: Relationship between coordinate systems for the inertial reference frame, \hat{n} , equilibrium frame, \hat{e} , and satellite body-fixed frame, \hat{b}

Modeling Methods

The controller is modeled using a variety of methods and operates under several assumptions and approximations. Some of these modeling techniques include state spaces and computer-aided analysis software such as AUTOLEV, MATLAB and Simulink. The controller assumes the satellite to be a constant mass system with constant moments of

inertia. The satellite's orbit is assumed to have zero eccentricity (i.e. perfectly circular), and the (sparse) atmosphere [8] through which the satellite moves is assumed to be uniform. Earth's gravitational influence on the satellite is assumed to be constant at all points along its orbit (i.e. perfectly spherical Earth with uniformly distributed mass). It is assumed that the satellite has no unexpected magnetic dipole moment acting on it; therefore, variations in Earth's magnetic field are of no consequence. Any disturbance torques and forces imparted on the satellite are assumed to be linear and nearly constant. The machinery within the satellite is assumed to generate no noise at all. As the satellite is in LEO, the solar pressure is insignificant relative to the larger forces due to aerodynamic drag and gravity gradient.

Deriving the Nonlinear Model

Variable Definitions

$\hat{b}_1, \hat{b}_2, \hat{b}_3$	Spacecraft's Principal Axes
$\hat{e}_1, \hat{e}_2, \hat{e}_3$	Flight Path's Equilibrium Axes
τ	Torque
$n = \sqrt{\frac{\mu}{R^3}}$	Mean Motion (constant)
N	Inertial Reference Frame
B	Satellite Body Reference Frame
State Vector: $\vec{x} = \begin{bmatrix} \phi \\ \theta \\ \psi \\ p \\ q \\ r \end{bmatrix}$	$\begin{bmatrix} roll \\ pitch \\ yaw \\ \omega \text{ about } \hat{b}_1 \\ \omega \text{ about } \hat{b}_2 \\ \omega \text{ about } \hat{b}_3 \end{bmatrix}$
Input Vector: $\vec{u} = \begin{bmatrix} u_1 \\ u_2 \\ u_3 \end{bmatrix}$	

To derive the equations of motion for a satellite attitude control system [7, 8], begin with the moment equation. Let S refer to the system, let B refer to the spacecraft's body, and let M refer to the spacecraft's momentum wheels.

$$M = \frac{d^N \vec{H}^S}{dt} \text{ where } {}^N \vec{H}^S = {}^N \vec{H}^B + {}^N \vec{H}^M$$

By the composite theorem, it follows that

$$M = \frac{d^N \vec{H}^S}{dt} = \frac{d^N \vec{H}^B}{dt} + \frac{d^N \vec{H}^M}{dt} \quad (1)$$

Apply the derivative theorem to find the angular momentum of the body. Let the angular velocity of the body be defined as

$${}^N \vec{\omega}^B = p \hat{b}_1 + (-n + q) \hat{b}_2 + r \hat{b}_3 \quad (2)$$

and assume that the following diagonal matrix is comprised of the principle moments of inertia

$$I_B = \begin{bmatrix} I_1 & 0 & 0 \\ 0 & I_2 & 0 \\ 0 & 0 & I_3 \end{bmatrix}$$

By the derivative theorem,

$$\dot{H}_B = \frac{^B d \vec{H}^B}{dt} + {}^N \vec{\omega}^B \times {}^N \vec{H}^B$$

$$\dot{H}_B = [I_B] {}^N \vec{\omega}^B + S({}^N \vec{\omega}^B) ([I_B] \cdot {}^N \vec{\omega}^B) \quad (3)$$

Consider the angular momentum of a spacecraft with momentum wheels, assuming constant angular momentum relative to the spacecraft:

$${}^B \vec{H}_R^e = H_{Rx} \hat{b}_1 + H_{Ry} \hat{b}_2 + H_{Rz} \hat{b}_3 \quad (4a)$$

and

$${}^N \vec{H}_R^e = -I_2 \hat{b}_2 + {}^B \vec{H}_R^e \quad (4b)$$

Since the desired outcome is to have the spacecraft maintain equilibrium, there must be a zero net torque on the entire spacecraft. Therefore, it follows that

$$-n \hat{b}_2 \times {}^N \vec{H}^e = -n \hat{b}_2 \times {}^B \vec{H}_R^e = n(H_{Rx} \hat{b}_1 - H_{Rz} \hat{b}_3) = 0$$

Thus, $H_{Rx} = H_{Rz} = 0$, and ${}^B \vec{H}_R^e = H_{Ry} \hat{b}_2$. This implies that there cannot be a momentum wheel on either the roll or the yaw axes for the spacecraft to properly maintain equilibrium. Additionally, it follows that ${}^N \vec{H}^M = {}^B \vec{H}_R^e$, and since this angular momentum is constant,

$${}^N \vec{H}^M = S({}^N \vec{\omega}^B)(H_{Ry}) \quad (5)$$

Next, when calculating the moments of a satellite attitude control system, the total sum of moments can be broken into two torques: the control torque, τ_C , generated by the reaction wheels, control moment gyro (CMG) arm, thrusters, and magnetic coils; and the disturbance torque, τ_D , generated by the aerodynamic drag, solar radiation, gravity gradient torque, magnetic field, and liquid propellant sloshing of the system. For the purpose of this study, all external torques besides the aerodynamic drag and the gravity gradient torque are assumed zero.

Similarly, control torques not generated by the reaction wheels are assumed zero.

To determine τ_D , first consider the aerodynamic component, τ_{Da} , which is approximately proportional to the angular perturbation of satellite pitch (θ) and yaw (ψ). Therefore, τ_{Da} can be written in terms of the aerodynamic stiffness matrix, D, such that

$$\tau_{Dg} = D(\theta, \psi)^T, \text{ where } D = \begin{pmatrix} L_\theta & L_\psi \\ M_\theta & M_\psi \\ N_\theta & N_\psi \end{pmatrix} \quad (6)$$

To calculate the gravity-gradient in LEO with an orbit of radius, R,

$$\tau_{Dg} = \int \rho \times a_g dm$$

where

$$\tau_{Dg} = \tau_{gx}\hat{b}_1 + \tau_{gy}\hat{b}_2 + \tau_{gz}\hat{b}_3 \quad (7)$$

and

$$\tau_{gx} = \frac{3}{2}n^2(I_3 - I_2) \cos^2(\theta)\sin(2\phi) \quad (7a)$$

$$\tau_{gy} = \frac{3}{2}n^2(I_3 - I_1) \cos^2(\phi)\sin(2\theta) \quad (7b)$$

$$\tau_{gz} = \frac{3}{2}n^2(I_1 - I_2) \sin(\phi)\sin(2\theta) \quad (7c)$$

When computing the control torque of the satellite control system, it is common to approximate the control torque as

$$\tau_c \cong [I_w]^N \dot{\Omega}^R \quad (8)$$

where the angular velocity of the reaction wheels is given by

$${}^N\bar{\Omega}^R = \Omega_1\hat{b}_1 + \Omega_2\hat{b}_2 + \Omega_3\hat{b}_3 \quad (9)$$

and $[I_w]$ is the matrix containing the principal moments of inertia for the reaction wheels. For this system, assume that the spin axes of the reaction wheels are perfectly aligned with the principal axes of the satellite's body; thus $[I_w]$ is a diagonal matrix. Furthermore, assume that the diagonal components of this matrix are all equal, and that the moment of inertia can be written as I_w .

To rewrite the control torque as the input vector, \vec{u} , let

$$u_1 = I_w \dot{\Omega}_1 \quad (10a)$$

$$u_2 = I_w \dot{\Omega}_2 \quad (10b)$$

$$u_3 = I_w \dot{\Omega}_3 \quad (10c)$$

Finally, substituting (3), (5), (6), (7), and (8) into (1), the first half of the nonlinear model is attained:

$$\tau_{Da} + \tau_{Dg} + \tau_c = [I_B]^N \bar{\omega}^B + S({}^N\bar{\omega}^B)([I_B] \bullet {}^N\bar{\omega}^B + H_{Ry}\hat{b}_2)$$

or

$$\begin{bmatrix} I_1 \dot{p} \\ I_2 \dot{q} \\ I_3 \dot{r} \end{bmatrix} = \tau_{Da} + \tau_{Dg} + \tau_c - S({}^N\bar{\omega}^B)([I_B] \bullet {}^N\bar{\omega}^B + H_{Ry}\hat{b}_2) \quad (11)$$

In solving for the remaining three variables in the specified state vector, it is important to note that the angular velocity of the body (2) can also be written in terms of the equilibrium velocity, $\omega^e = -n\hat{e}_2$, as

well as Euler's angles denoting roll, pitch, and yaw (φ, θ, ψ) :

$${}^N\bar{\omega}^B = -n\hat{e}_2 + \dot{\phi}\hat{b}_1 + \dot{\theta}\hat{b}_2 + \dot{\psi}\hat{b}_3 \quad (12)$$

To relate the equilibrium frame to the inertial reference frame, use the following Euler matrix:

$$\begin{bmatrix} \hat{e}_1 \\ \hat{e}_2 \\ \hat{e}_3 \end{bmatrix} = \begin{bmatrix} c_\theta c_\psi & -c_\theta s_\psi & s_\theta \\ c_\varphi s_\psi + c_\varphi s_\psi s_\theta & c_\varphi c_\psi - s_\varphi s_\psi s_\theta & -c_\theta s_\psi \\ s_\varphi s_\psi - c_\varphi c_\psi s_\theta & s_\varphi c_\psi + c_\varphi s_\psi s_\theta & c_\theta c_\varphi \end{bmatrix} \begin{bmatrix} \hat{b}_1 \\ \hat{b}_2 \\ \hat{b}_3 \end{bmatrix}$$

Then assuming small angle approximations,

$$\hat{e}_2 \cong \psi\hat{b}_1 + \hat{b}_2 - \phi\hat{b}_3$$

and equating the individual components of (2) and (12) it follows that,

$$\dot{\phi} = p + n\psi \quad (13)$$

$$\dot{\theta} = q \quad (14)$$

$$\dot{\psi} = r - n\phi \quad (15)$$

which serve as the first three equations of the state vector, \vec{x} .

Solving (11) for $\dot{p}, \dot{q}, \dot{r}$, and using equations (13), (14), and (15) yields the complete nonlinear model.

Linearization

In order to obtain a linear model for the system via the nonlinear model, it is common to assume small perturbation angles. Typically most models assume perturbation angles less than 45 degrees, but for the purpose of this linearization, assume that the angles φ, θ, ψ are approximately equal to zero. Additionally, assume that the angular velocity components p, q , and r are small, meaning the product of these terms are approximately equal to zero. After linearizing equations (11), (13), (14), and (15), the following linear model is used to represent the satellite attitude control system, and is written in the state-space form, $\dot{\vec{x}} = A\vec{x} + B\vec{u}$:

$$\begin{bmatrix} \dot{\phi} \\ \dot{\theta} \\ \dot{\psi} \\ \dot{p} \\ \dot{q} \\ \dot{r} \end{bmatrix} = \begin{bmatrix} 0 & 0 & n & 1 & 0 & 0 \\ 0 & 0 & 0 & 0 & 1 & 0 \\ -n & 0 & 0 & 0 & 0 & 1 \\ a_{41}a_{42}a_{43} & 0 & 0 & a_{46} & 0 & 0 \\ 0 & a_{52}a_{53} & 0 & 0 & 0 & 0 \\ 0 & a_{62}a_{63}a_{64} & 0 & 0 & 0 & 0 \end{bmatrix} \vec{x} + \begin{bmatrix} 0 & 0 & 0 \\ 0 & 0 & 0 \\ 0 & 0 & 0 \\ -1/I_1 & 0 & 0 \\ 0 & 1/I_2 & 0 \\ 0 & 0 & 1/I_3 \end{bmatrix} \vec{u}$$

where

$$a_{41} = \frac{3n^2(I_3 - I_2)}{I_1}$$

$$a_{42} = \frac{L_\theta}{I_1}$$

$$a_{43} = \frac{L_\Psi}{I_1}$$

$$a_{46} = \frac{n(I_3 - I_2) + H_{Ry}}{I_1}$$

$$a_{52} = \frac{M_\theta + 3n^2(I_3 - I_1)}{I_2}$$

$$a_{53} = \frac{M_\Psi}{I_2}$$

$$a_{62} = \frac{N_\theta}{I_3}$$

$$a_{63} = \frac{N_\Psi}{I_3}$$

$$a_{64} = \frac{n(I_2 - I_1) - H_{Ry}}{I_3}$$

Additionally, since the roll, pitch, and yaw angles are the desired output for this satellite attitude control system, the output can be written in the state space form, $\vec{y} = C\vec{x} + D\vec{u}$, where D is a 3×3 zero matrix, and C is the 3×6 matrix equal to:

$$C = \begin{bmatrix} 1 & 0 & 0 & 0 & 0 & 0 \\ 0 & 1 & 0 & 0 & 0 & 0 \\ 0 & 0 & 1 & 0 & 0 & 0 \end{bmatrix}$$

Additional Assumptions and Approximations

When considering the external disturbances on the system, it was assumed that the forces with predominant effects were the aerodynamic drag and the gravity gradient torque. As previously mentioned, other forces that act on this system are assumed zero. Since this particular system is simply a 1U CubeSat, it is logical to assume that the presence of any of the excluded external forces would render the mission a failure, as these forces would most likely destroy the satellite. Finally, the last assumption was that the mean motion, n , was constant and that there was zero deviation in the satellite's orbital radius as measured in relation to the center of the Earth.

Due to the many assumptions listed above, the linear model is a heavily reduced version of this nonlinear

system. Since this linear model is drastically simplified, there is reason to believe that the linear model does not accurately capture the full nonlinear response. As a result, to compare the accuracy of this linear approximation, the Linear Quadratic Controller (described in later sections) used to control this system is modeled using both the linear and the nonlinear system, and the response between these two models are compared. This allows an approximation in the error that results from the reduced linear model. The results presented here ultimately show that the linear model is an accurate representation for this nonlinear system.

Open Loop Simulation

This paper considers a 1U CubeSat orbiting in a perfectly circular orbit at 300km. CubeSats have a well-defined standard and usually have a volume of one liter, measurements of 10cm per side, and have a mass of no more than 1.33kg. Over 100 CubeSats have been launched into space since they were first introduced in 1999, and they are popular with schools due to their relatively low cost compared to traditional satellites [9]. The development of an attitude control system for this system is therefore of paramount importance if students and educators are to get meaningful scientific and engineering results from their satellites.

MATLAB and Simulink are utilized for model simulations [1,2]. Several parameters are required to fully define the system and are listed here:

$$\begin{aligned} I_1 &= 0.0017 \text{ kg/m}^2 \\ I_2 &= 0.0015 \text{ kg/m}^2 \\ I_3 &= 0.0020 \text{ kg/m}^2 \\ H_{Ry} &= 0.000625 \text{ N.m.s} \\ n &= 0.0011596575 \text{ rad/s} \\ L_\theta &= -5.1354 \times 10^{-11} \text{ N.m/rad} \\ M_\theta &= -8.559 \times 10^{-10} \text{ N.m/rad} \\ M_\Psi &= -1.7118 \times 10^{-11} \text{ N.m/rad} \\ N_\Psi &= -1.7118 \times 10^{-11} \text{ N.m/rad} \\ L_\Psi &= N_\theta = 0 \text{ N.m/rad} \end{aligned}$$

These values are appropriate for a 1U CubeSat with a circular orbit at an altitude of 300 km and with reaction wheels appropriate to its size [5]. Inserting these values into the aforementioned A and B matrices yields:

$$A = \begin{bmatrix} 0 & 0 & 1.15e-3 & 1 & 0 & 0 \\ 0 & 0 & 0 & 0 & 1 & 0 \\ -1.15e-3 & 0 & 0 & 0 & 0 & 1 \\ 1.18e-6 & -3.02e-8 & 0 & 0 & 0.367 & \\ 0 & 2.36e-7 & -1.14e-8 & 0 & 0 & 0 \\ 0 & 0 & -8.55e-9 & -3.120 & 0 & \end{bmatrix}$$

$$B = \begin{bmatrix} 0 & 0 & 0 \\ 0 & 0 & 0 \\ 0 & 0 & 0 \\ -588 & 0 & 0 \\ 0 & -666 & 0 \\ 0 & 0 & -500 \end{bmatrix}$$

A Simulink model can then be created to model the behavior of the system without a controller. Simple step functions are fed into each of the reaction wheels, and the response is observed.

Reaction wheels with a maximum torque of $6.35 \times 10^{-4} \text{ Nm}$ are used to control the satellite [6]. To test the response of the reaction wheels, a 5 second pulse of strength 10^{-5} Nm is sent through the reaction wheels in the ϕ , θ , and ψ directions, in that order, and the response is observed for 60 seconds. This causes oscillations in the nadir offset for the ϕ and ψ directions (due to the dynamic coupling between the two) and produces a linear decrease in the θ direction. A transient response is observed in the angular velocity perturbations for the ϕ and ψ directions, which settles into harmonic oscillations, while the angular velocity in the θ direction simply settles at another value when the pulse duration is complete (see Figure 2).

The naive assumption, that simply sending a pulse of negative amplitude after the initial pulse would return the system to steady pointing state, is incorrect. To confirm this, a 5 second pulse of strength -10^{-5} Nm is sent through each of the reaction wheels after sending the initial pulses. While the angular velocity in the θ direction can be restored to zero, it is much more difficult to restore the additional parameters of the system. Sending the additional pulse makes the angular velocity components oscillate with larger amplitude, as more energy is driven into the system rather than stabilizing it. The coupling between the ϕ and ψ directions makes restoring pointing and angular velocity to zero a difficult problem (see Figure 3).

As the model is inherently unstable, it is easy to send the system into a time-variant state. Restoring nadir pointing to the craft cannot be done simply and necessitates the inclusion of a control system.

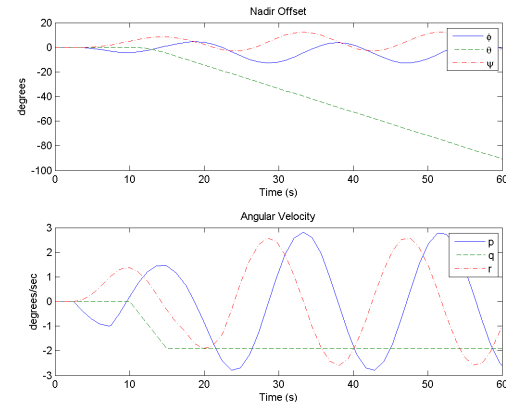


Figure 2: Observed response of the pointing position and angular velocities for a simple pulse.

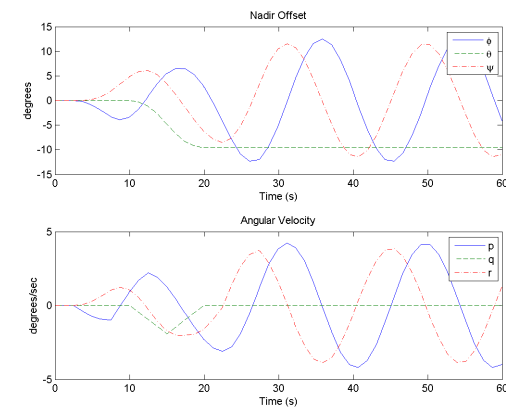


Figure 3: Observed response of the pointing position and angular velocities for the pulse/anti-pulse driver.

Controllability, Observability, and Stability

The controllability and observability of this system can be determined by solving for their respective matrices. By definition, the controllability matrix can be written as, $C = [B \ AB \ A^2B \ \dots \ A^{n-1}B]$ where this system's C matrix has dimension 6×18 . Since the $\text{rank}(C)=6$, this system is full row rank, and it can be concluded that this satellite attitude control system is controllable. To determine the observability of the system, compute the observability matrix

$$O = \begin{bmatrix} C \\ CA \\ CA^2 \\ \vdots \\ CA^{n-1} \end{bmatrix}$$

where the dimension of the observability matrix is equal to 18×6 and its corresponding rank is equal to 6. This system is maximum rank and is observable.

For a system to be stable, the eigenvalues of A must all have values less than zero. The eigenvalues of A were calculated to be:

$$\lambda(A) = \begin{bmatrix} -4.07e-15 + 3.39e-1i \\ -4.07e-15 - 3.39e-1i \\ 2.97e-10 + 1.16e-3i \\ 2.97e-10 - 1.16e-3i \\ 4.86e-4 \\ -4.86e-4 \end{bmatrix}$$

Since matrix A contains two eigenvalues that are greater than zero, this system is unstable. This was an expected result as the inclusion of the gravity gradient and the aerodynamic drag torques inherently makes this satellite unstable. For example, the gravity gradient torque is caused by the difference in the distances to Earth between the distinct points on the satellite's body, meaning the satellite will have a larger gravity gradient torque along the side that is closer to the Earth [19]. Similarly, the aerodynamic drag is a function of atmospheric density, the satellite's velocity, and the affected area, meaning the aerodynamic drag is implementing a continuous disturbance throughout the satellite's orbit [19]. Since these two external torques are changing with time throughout the satellite's orbit, their persistent pull on the satellite leads to an unstable system.

LQR Control Method

In many control applications, it is common to utilize a linear quadratic controller (LQR) as it allows the designer to select a cost function for controlling the system. For a LQR controller, the designer is allowed to allocate different weights to the state and input vectors, penalizing these vectors individually to minimize the stipulated cost function, and thus create an optimal controller [20, 21]. Since this system was already determined to be controllable, a LQR controller can be implemented to control nadir-offsets and de-tumbling.

For this satellite attitude control system, a cost function is defined as

$$J(u) = \int_0^{T_f} (x^T R x + u^T \Lambda u) dt \quad (16)$$

where $J(u)$ is a scalar value, R is a state penalty function matrix, Λ is an input penalty function matrix, x is the state vector, and u is the input vector. For a minimized LQR controller, both R and Λ are positive-definite, and thus by definition must have values greater than 0. When choosing R and Λ , there is a certain degree of relativity, and by making these

penalty functions diagonal matrices, the designer can penalize the use of specific inputs or states [21].

When the cost function (16) is minimized, the optimal input vector is calculated to be equal to

$$u_{optimal}(t) = -\Lambda^{-1} B^* P(t) x(t) \quad (17)$$

Then to solve for $P(t)$, the Riccati Equation states that

$$\dot{P}(t) = -P(t)A - A^*P(t) + P(t)B\Lambda^{-1}B^*P(t) - R$$

However, in assuming that this system is time-invariant, this cost function becomes an infinite-time LQR control problem, and the Riccati Equation is reduced to the Steady-State Riccati Equation

$$PA + A^*P - PBA^{-1}B^*P + R = 0$$

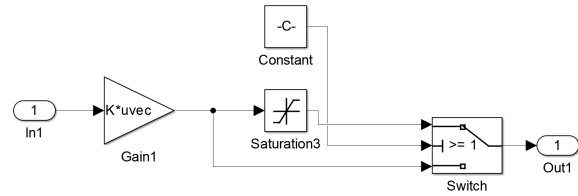


Figure 4: LQR controller modeled in Simulink.

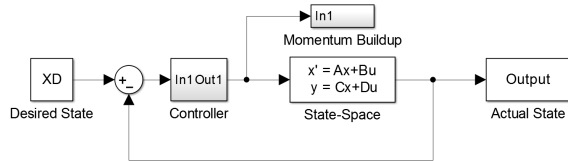


Figure 5: Linear model created in Simulink.

where P denotes P steady state, and the designer can now choose positive-definite penalty functions. Additionally, the optimal input vector can be rewritten as $u = -Kx$, where K is the optimal gain matrix, such that $K = \Lambda^{-1}B^*P(t)$. In utilizing Matlab's LQR function, the gain matrix K can be calculated, and allows the closed-loop control system model to be completed, see Figure 4 for LQR controller.

Design of the LQR controller began with a diagonal 6×6 L matrix multiplied by 1.0×10^{-3} , which represented the state penalty function that penalized all 6 states equally. Then the input penalty function, R , was chosen to be a diagonal 3×3 matrix so as not to penalize any of the inputs by a specific weight.

When applied to the linear model, given a 1.0 degree nadir-offset, the LQR controller allowed the satellite to return to equilibrium within 5.0 seconds, meeting the stipulated performance requirements. Similarly, when applied to the nonlinear model, the system also

returned from a 1.0 degree nadir-offset within the stipulated 5.0 second settling time. Both systems were able to recover from tumbling under 6.0 seconds, which is still within the performance requirements. Additionally, when both models were given a 90 degree nadir-offset along the roll axis, both models were able to recover under the allotted settling time, utilizing the L and R matrices specified above.

After reading additional articles that utilized aerodynamic forces to assist in de-tumbling, the designer developed a controller which proved to be the most efficient for this satellite system, where

$$L = \begin{bmatrix} 1 & 0 & 0 & 0 & 0 \\ 0 & 1 & 0 & 0 & 0 \\ 0 & 0 & 1 & 0 & 0 \\ 0 & 0 & 0 & 0 & 0 \\ 0 & 0 & 0 & 0 & 0 \\ 0 & 0 & 0 & 0 & 0 \\ 0 & 0 & 0 & 0 & 0 \end{bmatrix}, R = 10^4 * \begin{bmatrix} 1 & 0 & 0 \\ 0 & 1 & 0 \\ 0 & 0 & 1 \end{bmatrix}$$

This penalizes the attitude components of the state, and equally penalizes the inputs by a magnitude of 10^4 [20].

Performance Requirements

As previously mentioned, a satellite control system can be utilized for various applications. In order for a CubeSat to achieve optimal performance in any of these scenarios, it must de-tumble or return from a nadir-pointing error within a minimal amount of time. At comparable altitudes a passive satellite attitude control system can utilize aerodynamic forces to recover from a 10 deg/s tumble in approximately 5 hours [20]. For the purpose of this paper, the desirable recovery time from a nadir-pointing error or tumbling is approximately 7 seconds. While expecting a recovery from a small nadir-offset under 7 seconds is a reasonable goal, this performance requirement was then extended to see if this same 7 second settling time could be achieved under a large nadir-offset equal to 90 degrees along the roll axis.

In addition to stability requirements, this system must also meet the physical requirements of the satellite's respective hardware. This means the satellite must possess reaction wheels that saturate at about $6.35 \times 10^{-4} Nm$, and which have a maximum momentum buildup of $1.1 \times 10^{-3} Nms$ [5,6]. Throughout the testing process, all performance requirements were successfully achieved except in the case of a 90-degree nadir-pointing error.

Initial Conditions

In opposition to the linear design, the nonlinear initial conditions incorporate a non-trivial inertia matrix for the satellite and consider a full Euler matrix in determining the equations of state. Like the linear design, the nonlinear design first attempts to solve the regulator problem with all initial conditions zero and with nonlinear disturbances. However, unlike the linear model, small angles and an over-simplified satellite structure were not part of the nonlinear assumptions. Once the nonlinear design was found to be capable of resolving the regulator problem under zero initial conditions the initial pointing angle and angular velocities were modified in an attempt to ascertain the limits of the design.

In the initial design the satellite is assumed to have zero initial angular velocity. This condition was chosen under the pretext that a consumable method for de-tumbling the satellite after deployment had already been utilized. Since momentum reaction control continues to function only as long as the momentum actuators remain unsaturated, there is little point beginning in a state wherfrom recovery is impossible.

Additional design testing examined initial pointing perturbations (i.e. non-zero Euler angle states) of 1° and 90° and initial roll of 10% . These values were chosen to simulate various scenarios: 1) directional communications array pointing within acceptable deviation bounds, 2) recovery from highly perturbed orientation, and 3) recovery from tumbling.

Linear Model Results

A linear model of the system along with the LQR controller was built in Simulink (Figure 5). Three test cases were analyzed: a pointing error of 1 degree in each direction, a pointing error of 90 degrees along the roll axis, and a tumbling scenario of 10 degrees per second along the roll axis.

During the first test case, the pointing error of 1 degree along each primary axis, the system regained nadir pointing in less than 4 seconds with minimal overshoot. During recovery the craft reaches a maximum angular velocity of approximately 1 degree per second along each axis in less than 1 second, then quickly returns to equilibrium. The amplitudes of the attitude and angular velocities during this time can be seen in Figures 6 and 7, respectively. The reaction wheels respond to this offset with a maximum $2 \times 10^{-4} Nm$ torque in each wheel, leading to a final momentum buildup of the order $10^{-5} Nms$ along the ϕ and ψ directions, and approximately no buildup

along the θ axis. This level of momentum buildup is well within the physical limitations of the reaction wheels, $1.1 \times 10^{-3} Nms$. As the system returns to nadir within an amount of time less than our design specifications and does not break any of the mechanical limits of the chosen hardware, this test case meets the stipulated requirements.

In the second test case, the system regained nadir pointing in approximately 8 seconds with an overshoot of about 20 degrees. During recovery the craft reaches a maximum angular velocity of approximately 50 degrees per second along the roll axis. The amplitudes of the attitude and angular velocities during this time can be seen in Figures 8 and 9, respectively. The reaction wheels respond to this offset with an initial maximum torque in the ϕ and ψ directions followed by an oscillatory response which returns to zero at around 10 seconds (Figure 10).

While the steady state momentum buildup of the system is $10^{-3} Nms$ along the ψ direction and approximately $0 Nms$ along the ϕ and θ directions, the peak buildup is higher, $1.5 \times 10^{-3} Nms$. This value is above the maximum hardware constraints with the chosen reaction wheels. To accomplish this test case in the real world, passive stabilization (either by making use of the aerodynamic or gravitational torques, or perhaps the use of a magnetic damping system) would be required to bleed off some of the momentum buildup. Though the system returns to nadir within an amount of time less than our design specifications, it breaks the mechanical limits of the chosen hardware, and so fails our requirements.

In the final test case, a tumbling scenario of 10 degrees per second along the roll axis, the system returned to nadir pointing in approximately 4 seconds. In this scenario a maximum nadir offset of approximately 2.4 degrees is seen in the ϕ direction. Additionally the ϕ reaction wheel reaches saturation torque output for the first 0.5 second, and then trails back off to nothing after about 4 seconds. This leads to a final momentum buildup of $3 \times 10^{-4} Nms$, which is well within the allowed limit. This test case passes all of the requirements.

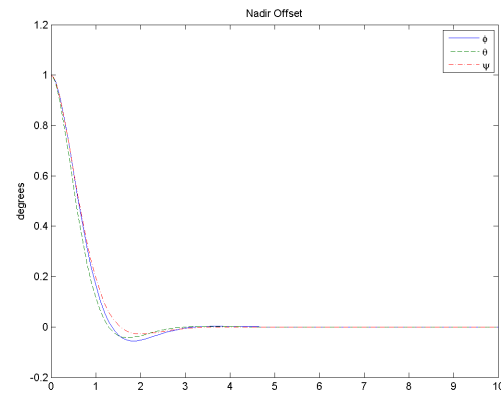


Figure 6: Observed response of the pointing position for the first test case.

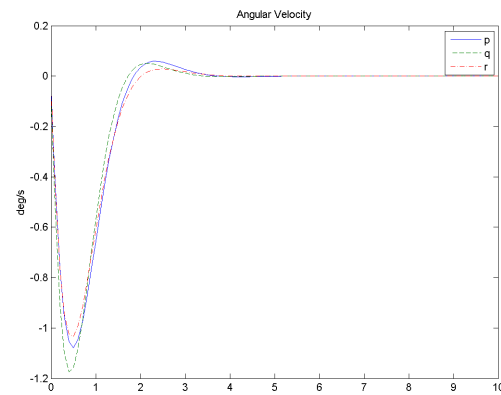


Figure 7: Observed response of the angular velocity for the first test case.

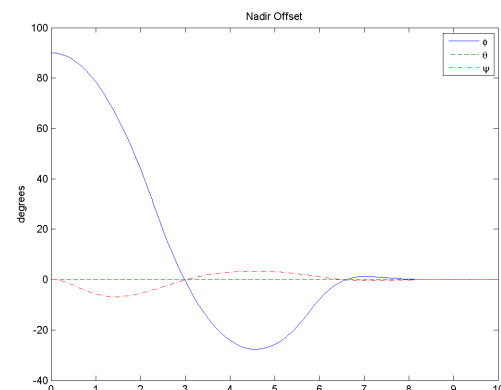


Figure 8: Observed response of the nadir offset for the second test case.

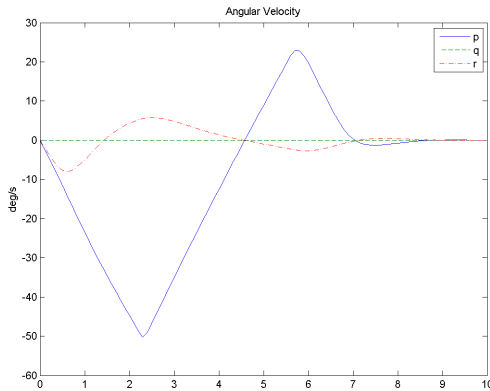


Figure 9: Observed response of the angular velocity for the second test case.

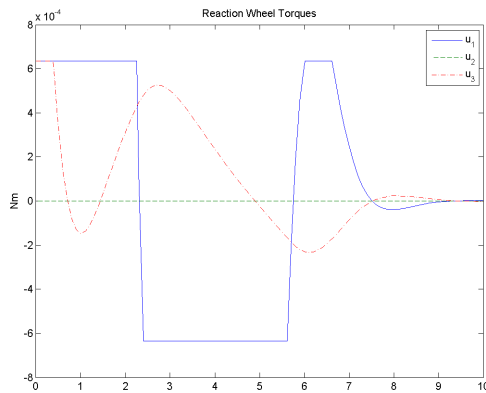


Figure 10: Observed response of the reaction wheel outputs for the second test case.

Observer Model Results

An observer model of the system along with the LQR controller was designed in Simulink (Figure 19) to test the system in the presence of noise. The state observer system provides an estimate of the internal state of the system from measurements of the input and output of the system. The sensor noise was generated with the use of Simulink's Band-Limited White Noise block, and the time history and distribution of the introduced noise can be seen in Figure 20. Sensors used to measure the attitude of CubeSats tend to have an accuracy of around 0.5 degrees, and so the white noise generator was tuned to produce noise of this magnitude. The sensors modeled sample at a rate of 10 Hz, which is appropriate considering those currently available [22].

The introduction to sensor noise in the system leads to a rather simple effect – the system can no longer be held at any constant value. Instead of being able to

absolutely say that the satellite is returned to nadir pointing, it can instead be said that the satellite is now within some range of values near nadir. The steady state behavior of the spacecraft is to oscillate around $\pm .06$ degrees of nadir at a rate of around $\pm .03$ degrees per second. This response is dictated by the reaction wheel response, which is of the order of $\pm 2 \times 10^{-6} Nm$, and leads to an oscillation in the momentum buildup of around $\pm 8 \times 10^{-7} Nms$. These values are acceptable for the chosen hardware. The use of an Observer is seen to be effective at minimizing the effects noise in the system outlined here.

Nonlinear Model and Results

The nonlinear equations governing the system were developed first and simplified to create a linear model. In designing the nonlinear model these equations were kept in their original form. The state parameters of interest were isolated and found in terms of the Euler angles and (angular) rates of change. These equations were used to build the foundation part of the nonlinear Simulink model.

From the Euler matrix and (12), the nonlinear angular velocity of the satellite body in the inertial reference frame is

$${}^N\bar{\omega}^B = [\dot{\phi} - n(c_\phi s_\varphi + c_\phi s_\theta s_\varphi)]\hat{b}_1 + [\dot{\theta} - n(c_\phi c_\varphi - s_\phi s_\theta s_\varphi)]\hat{b}_2 + (\dot{\varphi} + nc_\phi s_\varphi)\hat{b}_3$$

which, when set equal to (2), yields the following equations for $\dot{\phi}$, $\dot{\theta}$, and $\dot{\varphi}$:

$$\dot{\phi} = p + n(c_\phi s_\varphi + c_\phi s_\theta s_\varphi) \quad (18)$$

$$\dot{\theta} = q + n[(c_\phi c_\varphi - s_\phi s_\theta s_\varphi) - 1] \quad (19)$$

$$\dot{\varphi} = r - n(c_\theta s_\varphi) \quad (20)$$

Nonlinear design considers a non-trivial inertia matrix, which modifies the angular velocities about the satellite's body-centered axes. Angular accelerations \dot{p} , \dot{q} , and \dot{r} about these same axes are isolated from a slightly modified (11) wherein a new parameter $\tau_s = S({}^N\bar{\omega}^B)([I_B] \bullet {}^N\bar{\omega}^B + H_{Ry}\hat{b}_2)$ is introduced such that

$$\begin{bmatrix} I_{xx} & I_{xy} & I_{xz} \\ I_{yx} & I_{yy} & I_{yz} \\ I_{zx} & I_{zy} & I_{zz} \end{bmatrix} \begin{bmatrix} \dot{p} \\ \dot{q} \\ \dot{r} \end{bmatrix} = \tau_{Da} + \tau_{Dg} + \tau_C - \tau_s \quad (21)$$

Then, τ_s is found for each body-centered axis in terms of I , H , p , q , and r :

$$\begin{aligned}\tau_{sx} &= r(I_{yx}p - I_{yy}(n-q) + I_{yz}r + H_{ry}) \\ &\quad + (n-q)(I_{zx}p - I_{zy}(n-q) + I_{zz}r)\end{aligned}\quad (22)$$

$$\begin{aligned}\tau_{sy} &= p(I_{zx}p - I_{zy}(n-q) + I_{zz}r) \\ &\quad - r(I_{xx}p - I_{xy}(n-q) + I_{xz}r)\end{aligned}\quad (23)$$

$$\begin{aligned}\tau_{sz} &= (-n+q)(I_{xx}p - I_{xy}(n-q) + I_{xz}r) \\ &\quad - p(I_{yx}p - I_{yy}(n-q) + I_{yz}r + H_{ry})\end{aligned}\quad (24)$$

Multiplying both sides of (21) by the inverse inertia matrix, I^T , yields \dot{p} , \dot{q} , and \dot{r} .

Alternatively \dot{p} , \dot{q} , and \dot{r} may be found using Simulink and the form of the general equation – a method that turns out to be far less tedious than using the complex equations derived above (see Figure 11).

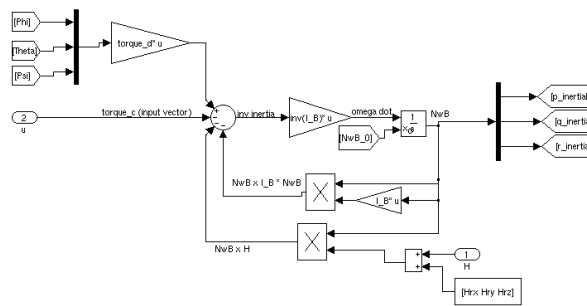


Figure 11: Simulink calculation of \dot{p} , \dot{q} , and \dot{r} .

As mentioned previously the design requirements were defined as a function of physical constraints and desired response time. For a 1U CubeSat the return-to-center performance requirement was a settling time of less than 7 seconds in all cases (small and large angle perturbation as well as tumbling). The largest torque and momentum that any single reaction wheel can accommodate is $6.35 \times 10^{-4} \text{ Nm}$ and $1.1 \times 10^{-3} \text{ Nms}$, respectively.

Figures 12 through 14 show that the performance requirement of a 7-second recovery time was met in the case of a small ($\phi_0 = \theta_0 = \varphi_0 = 1^\circ$) pointing error and modest tumbling rate ($p_0 = 10^\circ/\text{s}$) but not in recovering from a larger pointing errors ($\phi_0 = 90^\circ$), from which recovery takes nearly 10 seconds.

It is worth mentioning that, even though a 10-second recovery is beyond the performance specification, recovering from such a large perturbation in a still quite modest timespan is rather impressive.

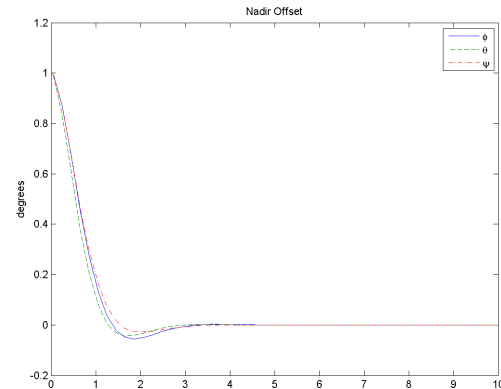


Figure 11: Recovery time from $\phi_0 = \theta_0 = \varphi_0 = 1^\circ$

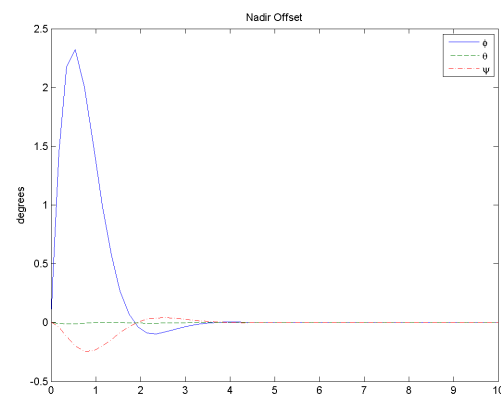


Figure 12: Recovery time from $p_0 = 10^\circ/\text{s}$

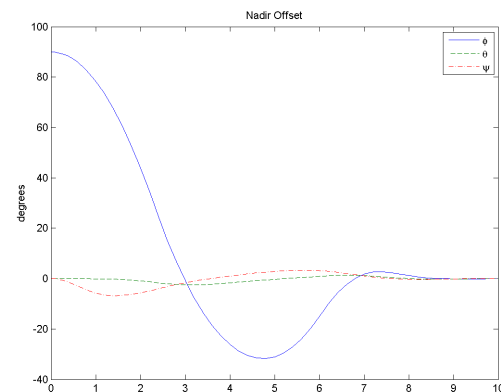
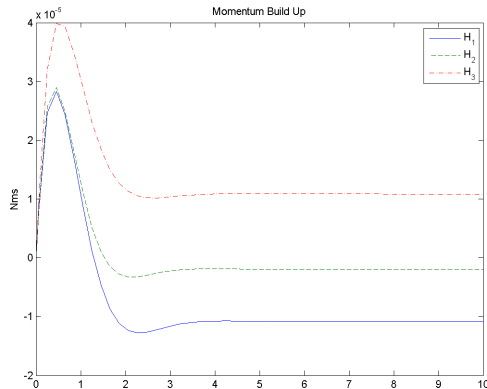
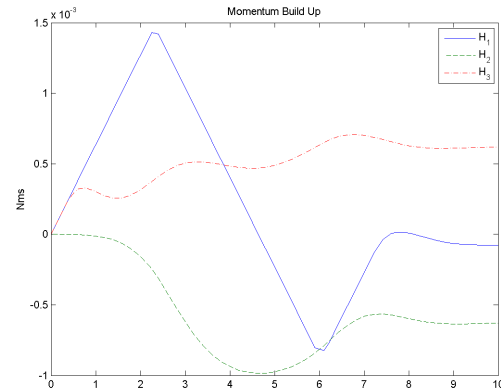
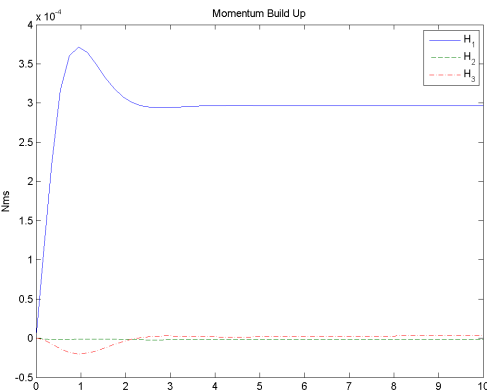
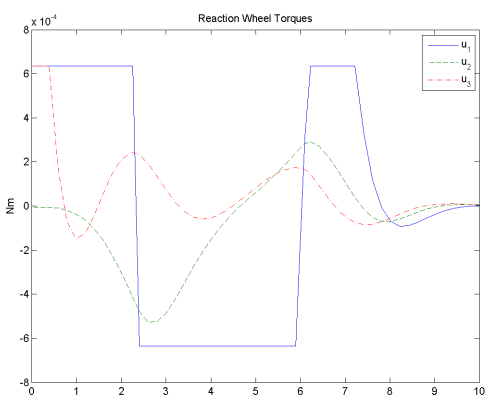


Figure 13: Recovery time from $\phi_0 = 90^\circ$

Figure 14: Momentum buildup from $\phi_0 = \theta_0 = \phi_0 = 1^\circ$ Figure 18: Momentum buildup from $\phi_0 = 90^\circ$ Figure 16: Momentum buildup from $p_0 = 10^\circ/\text{s}$ Figure 15: Reaction wheel torque from $\phi_0 = 90^\circ$

Another noteworthy figure is the maximum angular velocity observed amongst the three cases – almost $50^\circ/\text{s}$ in recovering from the 90° pointing error. For comparison, this rate is on par with angular velocities seen in a tumbling spacecraft [13].

With regard to the physical limitations of the system (i.e. maximum reaction wheel torque and momentum) the recovery from both the small nadir-pointing error and modest tumbling rate was well within respective maxima. These responses are shown in Figures 15 and 16.

In the case of recovery from a larger pointing error the controller again fell short of the performance requirement showing torque saturation in multiple reaction wheels and excessive momentum buildup (Figures 17 and 18), albeit temporary, in the roll-axis reaction wheel. The momentum buildup in this scenario (about $1.45 \times 10^{-3} \text{ Nms}$) is actually only slightly beyond the maximum allowable value.

It would be interesting to see how the controller would respond if it lost use of this reaction wheel (i.e. if momentum saturation was part of the model). An initial hypothesis, based on real-world reaction wheel failures, is that total loss of control along that (roll) axis would occur [4]. Control of that axis of rotation would not be restored until some energy was removed from the saturated wheel.

In cases where a reaction wheel becomes saturated before successfully reorienting the satellite it becomes necessary to dump momentum. Though quite gradual, one method through which a satellite in LEO can do so is via aerodynamic drag [19]. For small CubeSats, which are not typically equipped with thrusters or, if they are, carry little propellant, this form of passive momentum dumping is one of the only options. Another option is to dump

momentum via magnetism – that is, via charged rods that induce torque on the satellite by reacting with the magnetic field of the Earth (or some other body) [19].

One thing that the non-linear test cases highlight is the torque coupling that is evident between the roll and yaw reaction wheels. As an addendum to the original hypothesis of complete loss of rotational control upon same-axis reaction wheel saturation it might be possible to strategically “wiggle” some of the momentum onto unsaturated wheels to prevent saturation along the endangered axis. Additionally, in the linear model two reaction wheels become momentum-saturated in this case whereas this happens to only one in the nonlinear model.

Comparison to Other Models

A three-reaction wheel model has been used widely for creating attitude control systems for satellites [3, 4, 8, 10]. Further, reaction wheels are the primary and sometimes only method for attitude control for small satellites.

Other research has shown that reaction wheels can be used in the creation of controllers for various disturbances and uncertainties for 1U CubeSats. Attitude control of a satellite has been solved using MIMO quantitative feedback approaches, PID controllers relying on Hall sensor measurements, and various other control methods. Additionally, control research has been done in the control of larger, 2U and 3U controls [7, 10, 11, 12]. Reaction wheels were shown to be useful in controlling 3U CubeSats in the space dart configuration [13].

Similar results have been found using a PD control law to model reaction wheels to control the attitude of a CubeSat in a circular orbit. Initial attitude errors of 30 degrees were found to be correctable in as little as 20 seconds [14]. The LQR controller presented here is capable of restoring an initial error of 30 degrees in approximately 5 seconds, a substantial improvement to the PD controller.

Researchers have made use of magnetic rods and aerodynamic fins to stabilize CubeSats in low orbits. Using only the fins, attitude could passively be restored from a 90 degree offset to within 20 degrees in as little as 5 hours [19]. Making use of the fins and the magnetic dampeners resulted in the ability to stabilize a craft to within $\pm .25$ degrees in as little as 1 hour. While the reaction wheel approach taken in this paper provides response on a much shorter timescale, it was impossible to avoid oversaturating the momentum wheels for large pointing errors. The

use of aerodynamic fins would therefore be of great use for both passively stabilizing the craft and for the initial reorientation of the craft after launch, while the reaction wheels detailed above would be able to hold the craft more accurately than the magnetic dampening systems.

General Conclusions

Under normal circumstances (i.e. small pointing corrections and no tumbling) the linear and nonlinear models are almost identical – a claim supported by the scenario wherein a small nadir-pointing error is emulated. Considering the approximations (small angle, etc.) made in developing the linear model, which is based on nonlinear equations of state, this makes sense. Linear de-tumbling is also quite similar to that of nonlinear. The recovery time for both controllers in each of these scenarios is around 3 or 4 seconds – well within the performance requirements – while all wheels remain unsaturated. A slight difference in the form of torque coupling between the wheels on ψ and φ , the effects of which become even more obvious in case of large nadir-pointing error, exists between the two models.

Neither the linear nor the nonlinear model is capable of compensating for abnormally large pointing errors; however, the linear model, without torque coupling, ends up saturating two wheels trying to compensate for such an error. The nonlinear model splits enough momentum between the coupled axes that only the wheel on the third axis saturates.

In general, the controller designed herein is capable of very rapid response to orientation perturbations, which makes sense considering the size of the satellite and the physical characteristics of the reaction wheels. In an equilibrium, or near-equilibrium, scenario the linear controller provides more than adequate orientation stability. The errors due to simplification and approximation in the linear model may stack-up but a control system can compensate for this through regular recalibration.

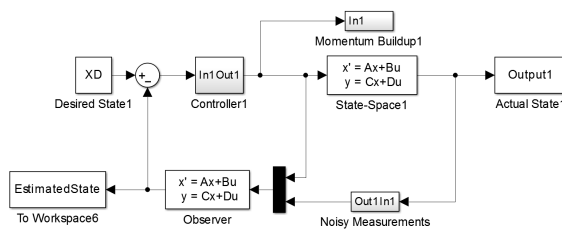


Figure 19: Observer model created in Simulink.

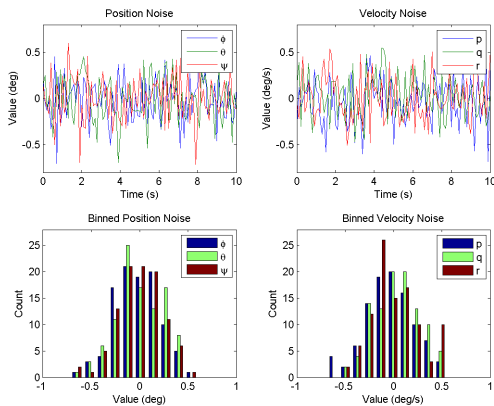


Figure 20: Noise input and distribution for the position and angular velocity sensors.

References

- [1] Simulink User's Guide, The Mathworks, 1992.
- [2] Mastering Simulink, Dabney and Harman, 2004.
- [3] Babcock, Erik. "CubeSat Attitude Determination via Kalman Filtering of Magnetometer and Solar Cell Data." (2011).
- [4] Kane, Thomas R., Peter W. Likins, and David A. Levinson. "Spacecraft Dynamics." New York, McGraw-Hill Book Co, 1983, 445 p. 1 (1983).
- [5] MAI-300 Single Axis Reaction Wheel, CubeSatShop.com, http://web.archive.org/web/20140421021522/http://www.cubesatshop.com/index.php?page=shop.product_details&flypage=flypage.tpl&product_id=92&category_id=7&keyword=momentum&option=com_virtuemart&Itemid=69
- [6] MAI-101 Miniature 3-Axis Reaction Wheel, CubeSatShop.com, http://web.archive.org/web/20140421021725/http://www.cubesatshop.com/index.php?page=shop.product_details&category_id=7&flypage=flypage.tpl&product_id=55&option=com_virtuemart&Itemid=69&vmcc_hk=1&Itemid=69
- [7] Nagi, Farrukh, et al. "Time-Optimal Satellite Attitude Bang-Bang Controllers." *Sign (s)* 8: 0.
- [8] Tewari, Ashish. Advanced Control of Aircraft, Spacecraft and Rockets. Vol. 36. John Wiley & Sons, 2011.
- [9] Nugent, Ryan, et al. "The cubesat: The picosatellite standard for research and education." *Aerospace Engineering* 805 (2008): 756-5087.
- [10] Nudehi, Shahin S., et al. "Satellite attitude control using three reaction wheels." *American Control Conference*, 2008. IEEE, 2008.
- [11] Snider, Ryan E. Attitude Control of a Satellite Simulator Using Reaction Wheels and a PID Controller. No. AFIT/GAE/ENY/10-M24. AIR FORCE INST OF TECH WRIGHT-PATTERSON AFB OH SCHOOL OF ENGINEERING AND MANAGEMENT, 2010.
- [12] Hoevenaars, Teun, Steven Engelen, and Jasper Bouwmeester. "Model-Based Discrete PID Controller for CubeSat Reaction Wheels Based on COTS Brushless DC Motors." *Advances in the Astronautical Sciences* 145 (2012): 379-394.
- [13] Armstrong, James, et al. "Pointing control for low altitude triple CubeSat space darts." (2009).
- [14] Oluwatosin, A.M.; Hamam, Y.; Djouani, K., "Attitude control of a CubeSat in a Circular Orbit using Reaction Wheels," *AFRICON*, 2013 , vol., no., pp.1,8, 9-12 Sept. 2013
- [15] Streetman, Brett, "Attitude Tracking Control Simulating the Hubble Space Telescope", 2003 (<http://www.dept.aoe.vt.edu/~cdhall/courses/aoe5984/bs.pdf>)
- [16] Zhang, Feng, et al., "Integrated relative position and attitude control of spacecraft in proximity operation missions with control saturation", Vol. 8 No. 5(B), 2012, ICIC International, ISSN 1349-3198
- [17] Hall, Chris, 2003, (unknown text), *Ch.4 Attitude Determination*, (<http://www.dept.aoe.vt.edu/~cdhall/courses/aoe4140/attde.pdf>)
- [18] Tudor, Zdenko, "Design and Implementation of Attitude Control for 3-axes Magnetic Coil Stabilization of a Spacecraft" (<http://www.diva-portal.org/smash/get/diva2:436730/FULLTEXT01.pdf>)
- [19] Rawashdeh, Samir A., "CubeSat Aerodynamic Stability at ISS Altitude and Inclination", *26th Annual AIAA/USU Conference on Small Satellites, 2012, Logan, UT*. Ed. SSC12-VIII-6 (<http://digitalcommons.usu.edu/cgi/viewcontent.cgi?article=1074&context=smallsat>)
- [20] Brathen, Gaute. "Design of Attitude Control System of a Double cubeSat." Norwegian University of Science and Technology, January 2013. (http://www.itk.ntnu.no/ansatte/Gravdahl_Jan.Tommy/Diplomer/Braaten.pdf)
- [21] Joshi, Sanjay. Lecture Notes, Mechanical and Aerospace Engineering 272. Davis, April 2013.
- [22] CubeSense, CubeSatShop.com, http://www.cubesatshop.com/index.php?page=shop.product_details&flypage=flypage.tpl&product_id=107&category_id=7&option=com_virtuemart&Itemid=69&vmcc_hk=1&Itemid=69